

# Design of a folded, conformationally stable oxaloacetate decarboxylase



Susan E. Taylor,<sup>a</sup> Trevor J. Rutherford<sup>b</sup> and Rudolf K. Allemann<sup>\*a</sup>

<sup>a</sup> School of Chemical Sciences, University of Birmingham, Edgbaston, Birmingham, UK B15 2TT. E-mail: r.k.allemann@bham.ac.uk; Fax: +44-121-414 4446;

Tel: +44-121-414 4359

<sup>b</sup> MRC-Centre for Protein Engineering, MRC Centre, Hills Road, Cambridge, UK CB2 2QH

Received (in Cambridge, UK) 3rd January 2002, Accepted 22nd February 2002

First published as an Advance Article on the web 12th March 2002

Oxaldie-4, a 31-residue polypeptide designed to catalyse the decarboxylation of oxaloacetate, has been synthesised and its structural and catalytic properties characterised. The solution structure of Oxaldie-4 was studied by CD and NMR spectroscopy. Oxaldie-4, the design of which was based on bovine pancreatic polypeptide, adopted a stably folded structure in solution, which was characterised by the tight packing of a poly-proline-like helix and an  $\alpha$ -helix as shown by a large number of inter-helix NOEs. The structure of Oxaldie-4 was in sharp contrast to the molten globule-like structure formed by Oxaldie-3, which was based on avian pancreatic polypeptide. The stability of Oxaldie-4 with respect to thermal and urea denaturation was significantly improved when compared to Oxaldie-3. Oxaldie-4 catalysed the decarboxylation of oxaloacetate with Michaelis-Menten saturation kinetics. The kinetic parameters, which were independent of the concentration of the catalyst over the whole range studied, were determined in a spectrophotometric assay at pH 7 and 298 K to be 0.229 s<sup>-1</sup>, 64.8 mM, and 2.9 M<sup>-1</sup> s<sup>-1</sup> for  $k_{\text{cat}}$ ,  $K_{\text{M}}$ , and  $k_{\text{cat}}/K_{\text{M}}$ , respectively. This catalytic efficiency corresponds to a rate increase of almost four orders of magnitude when compared to simple amines such as butylamine. However, despite the stable three-dimensional structure, the catalytic efficiency of Oxaldie-4 was only slightly improved relative to Oxaldie-3, most likely the consequence of the high flexibility of the lysine side chains, which make up the active site of Oxaldie-4.

## Introduction

The exquisite specificity and the remarkable catalytic efficiency of enzymes have long tempted chemists to design peptides that rival the efficiency of Nature's catalysts. True *de novo* design of enzymes has proved difficult<sup>1-3</sup> mainly because of our incomplete understanding of the biophysical basis of protein folding and stability and enzyme catalysis. Only in a few cases is the relationship between structure and reactivity at least partly understood. Oxaldie-1 and -2, peptides of 14 amino acid residues that aggregate and form amphiphilic  $\alpha$ -helices, catalyse the decarboxylation of oxaloacetate with significant rate enhancements.<sup>4,5</sup> The secondary structure was identified by NMR and CD-spectroscopy. However, due to the dynamic nature of the aggregates the tertiary structure could not be determined. Based on the design of SA-42, a short polypeptide which was shown by extensive spectroscopic studies to form a hairpin antiparallel helix-loop-helix dimer,<sup>6</sup> the construction of an oxaloacetate decarboxylase was reported.<sup>2</sup> The catalytic activity of this peptide was concentration dependent. Because folding was induced by dimerisation, concentrations in excess of 200  $\mu\text{M}$  were required for full activity. The peptide catalysed decarboxylation of oxaloacetate did not display Michaelis-Menten saturation kinetics and the catalytic efficiency was only one order of magnitude higher than that observed with simple amines such as butylamine.

The competing strategy of developing novel biocatalysts by making use of natural protein scaffolds such as catalytic antibodies and ribozymes has enjoyed considerable success.<sup>7-9</sup> The use of natural protein scaffolds like pancreatic polypeptide (PP) to present an array of functional groups to the substrate has been less successful, most likely because of the delicate stability of those peptides. Pancreatic polypeptide, peptide YY, and

neuropeptide Y constitute a family of C-terminally amidated peptides of 35 amino acids involved in the regulation of gastrointestinal function, blood pressure and feeding behaviour.<sup>10</sup> It has been postulated that the ability of these peptides to selectively bind and activate their respective receptors is critically dependent on their stable structure, the PP-fold. A crystal structure of avian PP (aPP) together with NMR structures of bovine PP (bPP) and peptide YY suggested that despite their small size all these peptides adopt similar stably folded structures in solution (Fig. 1).<sup>11,13</sup> The structure of aPP comprises a poly-proline type II helix (residues 1-8) and an  $\alpha$ -helix (residues 14-32).<sup>11</sup> The four residues at the C-terminus are highly mobile in solution and are not involved in the formation of the PP-fold. The poly-proline-helix and the  $\alpha$ -helix, which are joined by a type II  $\beta$ -turn, interact *via* hydrophobic contacts. Pancreatic polypeptides from different species as well as neuropeptide Y and peptide YY show approximately 50% sequence identity, which has been taken as evidence that all of these peptides share a similar structure. Indeed, the NMR structures of bPP and peptide YY showed that the overall fold of these two peptides was similar to that of aPP in the crystal structure with a RMS deviation of only 0.65 Å for the backbone atoms.<sup>12</sup> Therefore, these peptides appeared to provide an ideal scaffold for the design of proteins with catalytic<sup>14</sup> or DNA-binding<sup>15-17</sup> properties.

We have previously reported the design of Oxaldie-3 (Fig. 1A), a peptide which efficiently catalyses the decarboxylation of oxaloacetate through active site lysines, which we introduced into the solvent-exposed face of the  $\alpha$ -helix of aPP.<sup>14</sup> Surprisingly however, Oxaldie-3 displayed the typical characteristics of a molten globule. We now wish to report the structural and kinetic properties of Oxaldie-4, which was designed to contain the reactive lysine residues within the scaffold provided by bPP.

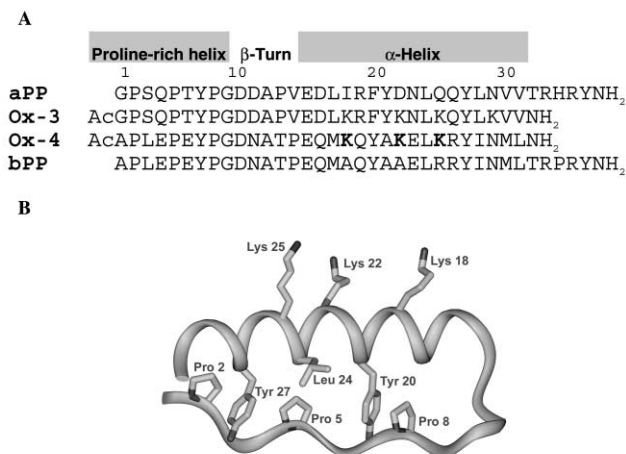


**Fig. 1** A, amino acid sequence alignment of aPP, bPP, Oxaldie-3 and Oxaldie-4 represented in the one-letter code. Amino acid residues, which are thought to contribute to the active site of Oxaldie-4, are shown in bold; B, structure of Oxaldie-4 as modelled based on the X-ray structure of aPP.<sup>11</sup> The side chains of the active site lysines protruding into the solvent are indicated. Side chains of some of the residues that make up the hydrophobic core between the poly-proline and the  $\alpha$ -helix are also shown.

The stabilities of Oxaldie-3 and -4 and their folding properties were strikingly different. The catalytic efficiency of Oxaldie-4 was increased approximately twofold relative to Oxaldie-3 and by almost four orders of magnitude relative to butylamine.

## Results and discussion

### Design and synthesis of Oxaldie-4

The design of Oxaldie-4 was based on the solution structure of bPP.<sup>12</sup> Three active site lysines were introduced on the solvent-exposed face of the  $\alpha$ -helix of bPP by replacing Ala 18, Ala 22, and Arg 25 (Fig. 1). Such a design should not disrupt either the interactions between the poly-proline helix and the  $\alpha$ -helix nor the hydrophobic core formed in the dimer at the interface between the subunits. In order to stabilise the helices the peptide was designed as the C-terminal amide and with an acetylated N-terminus.

Oxaldie-4 was synthesised by solid-phase peptide synthesis using standard Fmoc chemistry, purified by C18 reverse phase HPLC and identified by MALDI and electrospray mass spectrometry. The experimentally observed mass was identical to the calculated mass of 3680.

### Structural characterisation of Oxaldie-4

The circular dichroism spectrum of Oxaldie-4 was that which is typical of pancreatic polypeptides with minima at 208 nm and 222 nm but with slight distortions relative to the CD spectra of purely  $\alpha$ -helical peptides (Fig. 2A).<sup>18,19</sup> It was comparable to the CD spectra measured for Oxaldie-3 and bovine and avian PP.<sup>14,18,19</sup> The spectrum of Oxaldie-4 was independent of the peptide concentration for the whole range studied (1–200  $\mu$ M).

The behaviour of Oxaldie-4 with respect to thermal denaturation was different from that observed for Oxaldie-3. While isodichroic points at 204 and 238 nm were observed for both peptides (Fig. 2A),<sup>14</sup> suggesting two-state equilibria between the folded and denatured state, the shapes of the thermal denaturation curves were significantly different. The thermal denaturation of Oxaldie-4 showed a relatively sharp unfolding transition with a melting temperature of 50  $^{\circ}$ C (Fig. 2B). Considering the small globular shape of Oxaldie-4, the high melting temperature is remarkable and suggests a compact structure. On the other hand, the melting temperature measured for Oxaldie-3 was 34  $^{\circ}$ C and the flatness of the melting curve of Oxaldie-3 had been interpreted as indicative of reduced co-operativity in

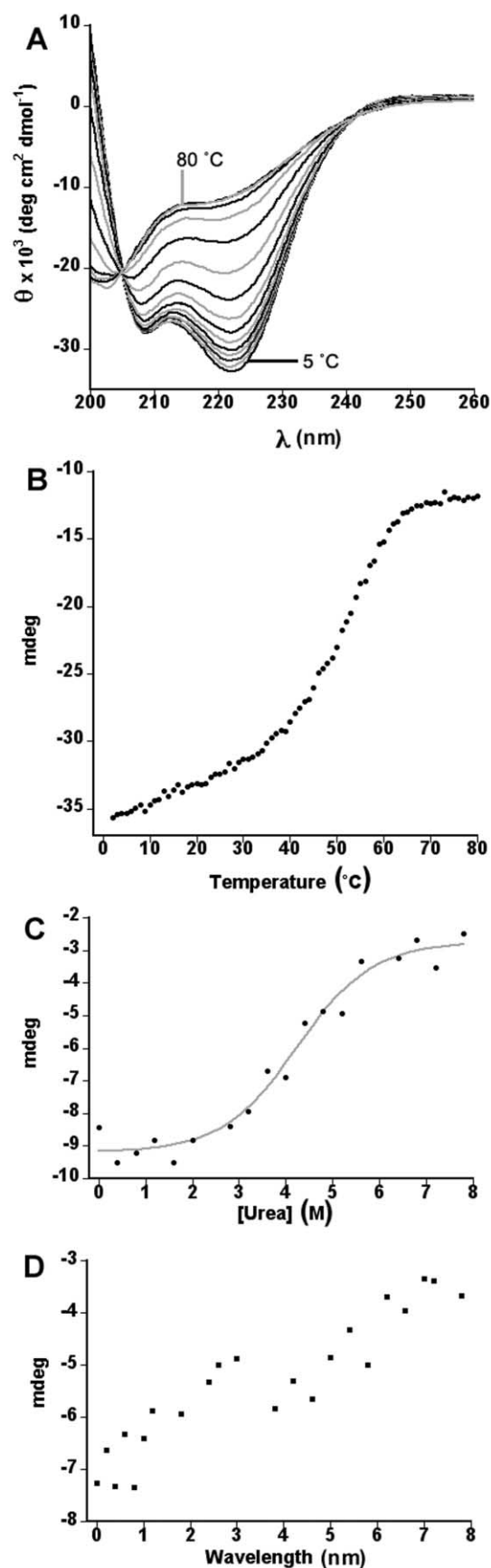


**Fig. 2** A, CD-spectra for a thermal denaturation experiment of 21.4  $\mu$ M Oxaldie-4 in 1 mM potassium phosphate (pH 7) and 10 mM NaClO<sub>4</sub> between 5  $^{\circ}$ C and 80  $^{\circ}$ C; B, thermal denaturation of Oxaldie-4 (21.4  $\mu$ M in 1 mM potassium phosphate, pH 7, and 10 mM NaClO<sub>4</sub>), depicted as a plot of the measured ellipticity at 222 nm versus temperature; C and D, urea unfolding of Oxaldie-4 (27.1  $\mu$ M) and Oxaldie-3 (19.5  $\mu$ M) in 1 mM potassium phosphate (pH 7) and 10 mM NaClO<sub>4</sub> at 25  $^{\circ}$ C; the measured ellipticity at 222 nm is plotted against the concentration of urea.

the unfolding reaction.<sup>14</sup> The gradual decrease of the helical content of Oxaldie-3 with increasing temperature was typically that of a molten globule state. It is interesting to note that the CD-spectra of both Oxaldie-3 and -4 are not those of fully denatured proteins even at 80 °C (Fig. 2A).<sup>14</sup>

Similarly, Oxaldie-3 and Oxaldie-4 behaved qualitatively differently in urea denaturation experiments. The denaturation curve of Oxaldie-4 was sigmoidal as expected for a stably folded protein (Fig. 2C). The concentration of urea at which 50% of Oxaldie-4 was denatured was determined to be 4.26 M from the denaturation curve. Experimentally it has been shown that there is a linear relationship between the free energy of unfolding a protein in the presence of urea and the concentration of the denaturant,<sup>20–22</sup> eqn. (1).

$$\Delta G_{U-F}^D = \Delta G_{U-F}^{H_2O} - m_{U-F}[D] \quad (1)$$

From the measurement of the ellipticity at 222 nm for Oxaldie-4 as a function of the concentration of urea, the free energy of unfolding in water  $\Delta G_{U-F}^{H_2O}$  and  $m_{U-F}$ , a constant which is proportional to the increase in the degree of exposure of the protein on denaturation, could be estimated as  $-2.76$  kcal mol<sup>-1</sup> and  $0.65$  kcal mol<sup>-1</sup>, respectively. The behaviour of Oxaldie-3 was very different and the free energy of unfolding could not be determined.<sup>14</sup> Its denaturation curve was not sigmoidal. The ellipticity at 222 nm (and therefore the decrease of the  $\alpha$ -helical content) decreased in an almost linear fashion with increasing concentrations of urea (Fig. 2D).

NMR experiments with Oxaldie-4 confirmed that the peptide adopted a stably folded conformation. <sup>1</sup>H Homonuclear TOCSY and NOESY spectra of Oxaldie-4 in H<sub>2</sub>O were run for resonance assignment and structural characterisation. The complete sequence-specific assignment was assisted by use of both the sequential amide proton NOEs and the close similarity to the chemical shift assignment in bPP.<sup>12</sup> In contrast with the <sup>1</sup>H-chemical shifts observed for Oxaldie-3,<sup>14</sup> a significant dispersion in the amide proton chemical shifts of Oxaldie-4, similar to the extent of dispersion in native bPP, was immediately evident in the TOCSY experiment indicating the formation of secondary structure. Most spin systems in Oxaldie-4 for amino acids of a common type were resolved. Sequence-specific assignment of the three lysine side chains, which were not present in native bPP, was accomplished by NH–NH NOE correlations. A 2D <sup>1</sup>H, <sup>13</sup>C HSQC–TOCSY spectrum was useful for confirming assignments, particularly using the characteristic threonine <sup>13</sup>C chemical shifts. Pro 8 in Oxaldie-4 exhibited poorly resolved <sup>1</sup>H signals. All four proline C $\alpha$  resonances were identified above 60 ppm in the HSQC–TOCSY, and each showed connectivities to H $\alpha$  and H $\beta$  resonances. The remaining <sup>1</sup>H assignments for Pro 8 were obtained by close inspection of the TOCSY.

Oxaldie-4 exhibited in excess of 100 NOEs between aliphatic protons and protons in the NH/aromatic region that did not overlay with TOCSY cross-peaks (Fig. 3A). The NH–NH region of the NOESY spectrum for Oxaldie-4 showed strong, clearly resolved sequential NOE cross peaks (Fig. 3B). Clearly resolved  $d_{NN}(i, i + 1)$  NOE cross-peaks were observed. In addition, all medium range  $d_{\alpha N}(i, i + 3)$  NOEs were evident in the segment 14–28 indicative of stable  $\alpha$ -helix formation in the C-terminal region (Fig. 4). These non-sequential NOEs were absent from residues 1–13, although four residues in this N-terminal region were prolines lacking the NH proton. For each of the four proline residues strong  $d_{\alpha N}(i, i - 1)$  NOEs were evident indicating that these proline amide bonds were in the *trans*-conformation. Several long range NOEs were observed. For example, the side chain of Tyr 27 could be correlated with the side chains of Pro 2, Glu 4, Pro 5 and Glu 6. Strong NOEs were also observed between Tyr 20 and Pro 5, Glu 6 and Pro 8 and between the side chains of Pro 5 and Leu 24. These NOEs between residues of the poly-proline helix and aromatic or

aliphatic residues of the  $\alpha$ -helix confirmed the presence of a tertiary structure similar to that of bPP (Fig. 1). The CD and NMR data presented herein clearly showed that the conformational properties of Oxaldie-3 and Oxaldie-4 in solution were different. Oxaldie-4 exhibited stable secondary and tertiary structure, resembling that of native bPP. Oxaldie-3, on the other hand, was only loosely compacted and appeared to be in a molten globule-like state.<sup>14</sup> It is possible that in solution the parent proteins avian and bovine PP also display similar differences in their conformational stability.

### Catalytic properties of Oxaldie-4

The Oxaldie-4 catalysed decarboxylation of oxaloacetate was studied by UV spectroscopy in a coupled enzymatic assay.<sup>1</sup> Rates for the decarboxylation of oxaloacetate to produce pyruvate were obtained from measuring the rate of conversion of NADH to NAD<sup>+</sup> in the lactate dehydrogenase-mediated conversion of pyruvate to lactate. The Oxaldie-4 catalysed reaction observed Michaelis-Menten kinetics with  $k_{cat} = 0.229$  s<sup>-1</sup> and  $K_M = 64.8$  mM and a catalytic efficiency  $k_{cat}/K_M$  of  $2.9$  M<sup>-1</sup> s<sup>-1</sup> (Table 1). The catalytic efficiency of Oxaldie-4 was independent of the peptide concentration for the whole range studied (4–40  $\mu$ M) as would be expected for a peptide with enzyme-like behaviour. The catalytic efficiency of Oxaldie-4 was improved approximately twofold relative to Oxaldie-3 (Table 1). The fluctuating tertiary structure of molten globules may have suggested that improving the stability of the protein fold should have led to a significant increase in the catalytic efficiency of the peptide. However, because the molten globule state of Oxaldie-3 is characterised by a compactness similar to that of the native state with native-like secondary structure, the high flexibility of the lysine side chains, which make up the active sites, is most likely the explanation for the similar catalytic properties of Oxaldie-3 and -4.

In summary, changing the backbone from that of avian to that of bovine PP resulted in the conversion of a molten globule (Oxaldie-3) to a stably folded peptide (Oxaldie-4) with a well-defined three-dimensional structure with slightly improved catalytic efficiency. It is commonly assumed that homologous proteins adopt similar conformations in solution and the different properties of Oxaldie-3 and -4 may therefore be surprising. 14 of the 31 amino acids are identical and several of the non-identical residues are replaced in a conservative fashion. In medium to large size proteins this level of similarity would be considered quite high. However, due to the much smaller number of interactions that determine the folded structure of small peptides such as the 31 residue Oxaldie-3 and -4, small changes in their primary sequence can clearly have dramatic effects on the stability of the folded conformation. Investigations are under way to define the key determinants of the different stabilities of Oxaldie-4 and Oxaldie-3 and indeed of bPP and aPP.

## Experimental

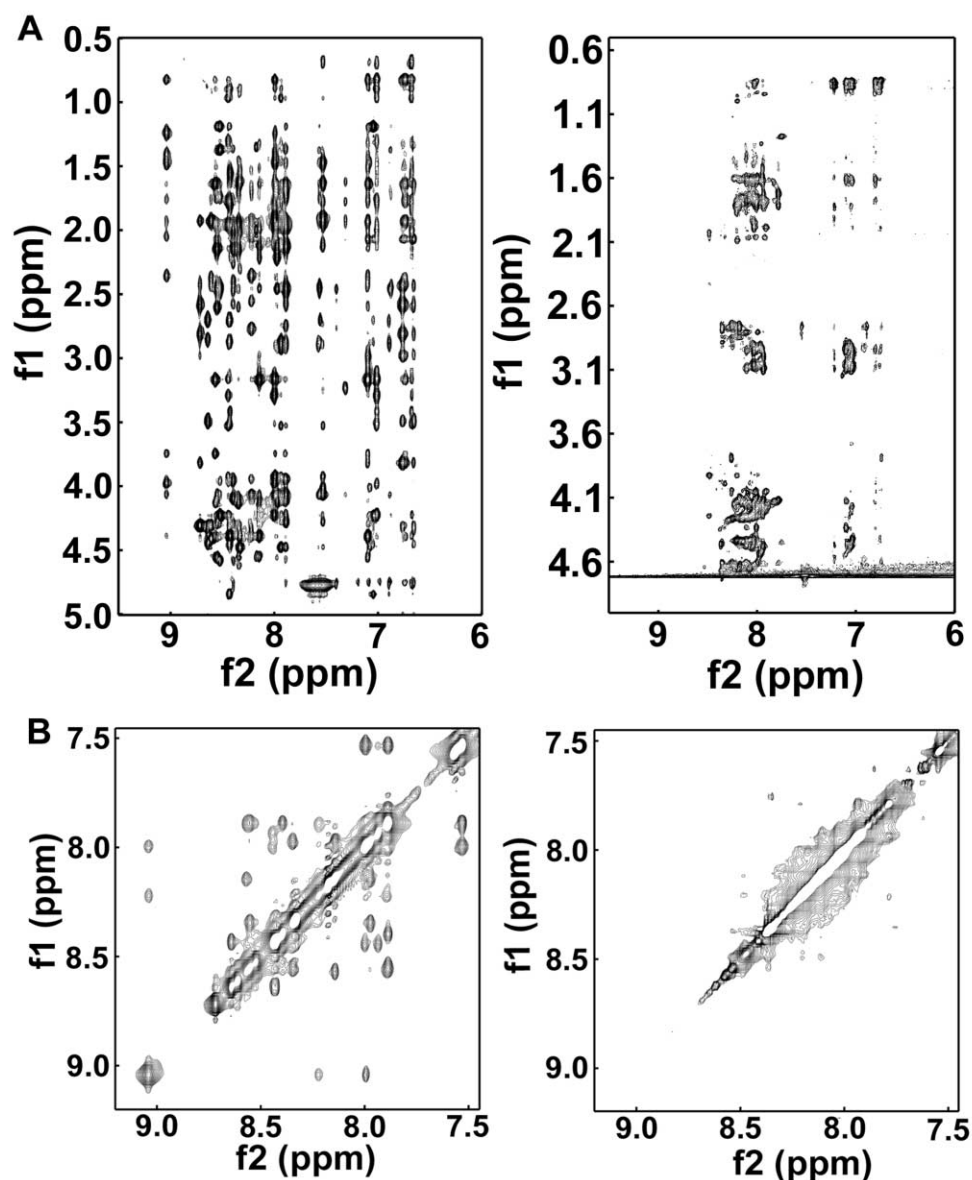
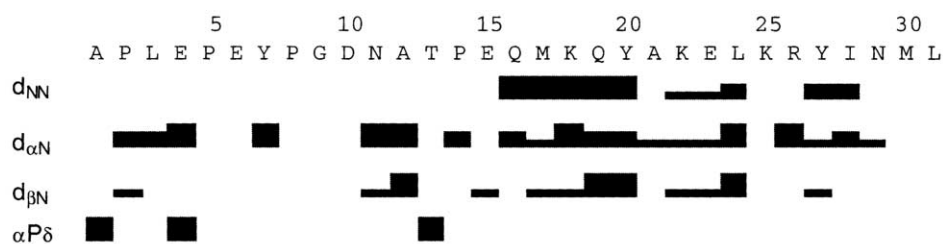
### Peptide synthesis, purification and identification

Oxaldie-4 was synthesised on Fmoc-5-(4-aminomethyl-3,5-dimethoxyphenoxy)valeric acid (PAL) on a polyethylene glycol grafted polystyrene support using a Pioneer Perceptive Biosystems automated peptide synthesiser and standard Fmoc protocols. The following protected amino acids were used: Fmoc-L-Asn (Tr), Fmoc-L-Thr (Bu'), Fmoc-L-Gln (Tr), Fmoc-L-Asp (OBu'), Fmoc-L-Arg (Pbf), Fmoc-L-Lys (Boc), Fmoc-L-Ser (Bu'), Fmoc-L-Glu (OBu'), Fmoc-L-Tyr (Bu'). The N-terminal amine was reacted with acetic anhydride after peptide assembly and prior to peptide cleavage.

The peptide was cleaved from the polymer and deprotected in 2 ml of 88% TFA, 5% water, 5% phenol and 2% triisopropylsilane per 0.2 g of resin for 2 hours at room temperature. The

**Table 1** Comparison of the kinetic parameters for the decarboxylation of oxaloacetate with Oxaldie-3 and Oxaldie-4 and *n*-butylamine in 50 mM BES (pH 7) and 10 mM NaCl at 298 K

Catalyst	[Cat]/ $\mu\text{M}$	$k_{\text{cat}}/10^{-3} \text{ s}^{-1}$	$K_{\text{M}}/\text{mM}$	$(k_{\text{cat}}/K_{\text{M}})/\text{M}^{-1} \text{ s}^{-1}$
Oxaldie-4	4–40	229	64.8	2.9
Oxaldie-3	5–40	86	49.4	1.74
BuNH <sub>2</sub>				0.0005
Spontaneous		0.013		

**Fig. 3** A, comparison of the NH-aliphatic regions of the NOESY spectra of Oxaldie-4 (left) and Oxaldie-3 (right) recorded in 90% H<sub>2</sub>O–10% D<sub>2</sub>O at 298 K with a NOE mixing time of 200 ms; B, NH–NH regions of the 200 ms NOESY spectra of Oxaldie-4 (left) and -3 (right).**Fig. 4** Amino acid sequence of Oxaldie-4 and summary of all the short-range NOEs involving the NH, C <sub>$\alpha$</sub> H and C <sub>$\beta$</sub> H. The NOEs are classified as strong, medium or weak as indicated by the thickness of the lines.

resin was removed and the peptide solution concentrated *in vacuo*. After diethyl ether precipitation and lyophilisation from 10% acetic acid, the peptide was redissolved in DMSO and

purified by reverse-phase HPLC on a preparative LUNA 10  $\mu$  C<sub>18</sub> (2) column (250 mm  $\times$  21.6 mm). The peptide was eluted following a linear gradient from 24% acetonitrile in water

(0.05% TFA) to 31% acetonitrile in water (0.05% TFA) over 90 minutes increasing to 33% acetonitrile over the next 30 minutes with a flow rate of 6 ml min<sup>-1</sup> and UV detection at 210, 215, 230 and 280 nm. Oxaldie-4 eluted at 32% acetonitrile. The solvent was removed *in vacuo*. The peptide was lyophilised twice from water and identified by electrospray and MALDI-TOF mass spectrometry. The obtained molecular mass was within 1 au of the calculated mass. No high molecular mass impurities could be detected. The purity of Oxaldie-4 was estimated to be more than 95% from HPLC on an analytical LUNA 10  $\mu$  C<sub>18</sub> (2) column (250 mm  $\times$  4.6 mm) and from electrospray mass spectrometry.

### NMR spectroscopy

Oxaldie-4 was prepared as a 4.9 mM (10 mg in 0.55 ml) solution in unbuffered 90% H<sub>2</sub>O-10% D<sub>2</sub>O. The spectra changed only insignificantly with pH between 3.0 and 5.6. <sup>1</sup>H-<sup>1</sup>H TOCSY and NOESY spectra were recorded using standard pulse sequences and WATERGATE solvent suppression, running on a Bruker Avance 800 MHz spectrometer. The TOCSY was acquired with 55 ms DIPSI-2 spin lock in a 6.25 kHz B<sub>1</sub> field, and processed with cosine-bell weighting to give a final resolution of 4.7 and 9.4 Hz per point in *f*<sub>2</sub> and *f*<sub>1</sub>, respectively. The NOESY was acquired with 200 ms NOE mixing time, and processed with cosine-bell weighting to give a final resolution of 4.7 and 9.4 Hz per point in *f*<sub>2</sub> and *f*<sub>1</sub>. All spectra were recorded with a nominal probe temperature of 298 K.

### CD spectroscopy

Circular dichroism experiments were run for samples in 1 mM potassium phosphate (pH 7) and 10 mM NaClO<sub>4</sub> at 20 °C in the wavelength interval 190–300 nm using a Jasco J-810 spectropolarimeter. The experiments were carried out in 1, 5 and 10 mm cells. The temperature dependence of the CD spectra was measured using a water-jacketed cell together with a programmable recirculating water bath. The temperature was increased from 2 °C to 80 °C with a slope of 20 °C per hour.

For urea denaturation experiments a stock solution of 800  $\mu$ M peptide in 1 mM potassium phosphate (pH 7) was diluted through the addition of the appropriate volume of a solution of 8 M urea in phosphate buffer to reach a final peptide concentration of 20  $\mu$ M and concentrations of urea ranging from 0 to 7.4 M. All samples were then equilibrated at 25 °C for 16 h. The CD spectra were measured at 25 °C using 1 mm cuvettes.

### Kinetic measurements

The kinetic experiments were carried out using a Shimadzu UV-2401PC UV-VIS spectrophotometer equipped with a Shimadzu temperature controller essentially as described.<sup>1,5</sup> Briefly, the rate of formation of pyruvate in Oxaldie-4 catalysed decarboxylations of oxaloacetate was measured at 298 K in 50 mM *N,N*-bis(2-hydroxyethyl)-2-aminoethanesulfonic acid (pH 7)-10 mM NaCl using lactate dehydrogenase by following the decrease of the absorbance of NADH (0.2 mM) at 340 nm ( $\epsilon = 6.23 \times 10^3 \text{ M}^{-1} \text{ cm}^{-1}$ ) in aliquots first treated with malate

dehydrogenase (necessary because all commercial preparations of lactate dehydrogenase contain malate dehydrogenase). Concentrations of oxaloacetate were between 0.75 and 218 mM. Peptide concentrations were determined by quantitative amino acid analysis. The kinetic parameters were determined with the program Sigma Plot.

### Abbreviations

aPP, avian pancreatic polypeptide; BES, *N,N*-bis(2-hydroxyethyl)-2-aminoethanesulfonic acid; bPP, bovine pancreatic polypeptide; Pbf, 2,2,4,6,7-pentamethylidihydrobenzofuran-5-ylsulfonyl; PP, pancreatic polypeptide.

### Acknowledgements

This work was supported by a BBSRC grant (RKA) and by the School of Chemical Sciences. We thank Dr Peter R. Ashton, Neil Spencer, and Graham Burns for help with mass spectrometry, NMR spectroscopy, and the purification of peptides.

### References

- 1 K. Johnson, R. K. Allemann, H. Widmer and S. A. Benner, *Nature*, 1993, **365**, 530.
- 2 M. Allert, M. Kjellstrand, K. Broo and L. Baltzer, *J. Chem. Soc., Perkin Trans. 2*, 1998, 2271.
- 3 J. Nilson and L. Baltzer, *Chem. Eur. J.*, 2000, **6**, 2214.
- 4 R. K. Allemann, PhD Thesis ETH, Zurich, 1989.
- 5 K. Johnsson, PhD Thesis ETH, Zurich, 1992.
- 6 S. Olofsson, G. Johansson and L. Baltzer, *J. Chem. Soc., Perkin Trans. 2*, 1995, 2047.
- 7 P. G. Schultz and R. A. Lerner, *Science*, 1995, **269**, 1835.
- 8 A. J. Kirby, *Acta Chem. Scand.*, 1996, **50**, 203.
- 9 D. P. Bartel, in *The RNA World*, 2nd edn., eds. R. F. Gesteland, T. R. Chech and J. F. Atkins, Cold Spring Harbor Laboratory Press, Cold Spring Harbor, New York, 1992.
- 10 L. Grundemar, in *Neuropeptide Y and Drug Development*, eds. L. Grundemar and S. R. Bloom, Academic Press, San Diego, 1997, pp. 1–14.
- 11 T. L. Blundell, J. E. Pitts, I. J. Tickle, S. P. Wood and C.-W. Wu, *Proc. Natl. Acad. Sci. USA*, 1981, **78**, 4175.
- 12 X. Li, M. J. Sutcliffe, T. W. Schwartz and C. M. Dobson, *Biochemistry*, 1992, **31**, 1245.
- 13 D. A. Keire, M. Kobayashi, T. E. Solomon and J. R. Reeve, Jr., *Biochemistry*, 2000, **39**, 9935.
- 14 S. E. Taylor, T. J. Rutherford and R. K. Allemann, *Bioorg. Med. Chem. Lett.*, 2001, **11**, 2631.
- 15 N. J. Zondlo and A. Schepartz, *J. Am. Chem. Soc.*, 1999, **121**, 6938.
- 16 J. W. Chin and A. Schepartz, *J. Am. Chem. Soc.*, 2001, **123**, 2929.
- 17 J. W. Chin, R. M. Grotzfeld, M. A. Fabian and A. Schepartz, *Bioorg. Med. Chem. Lett.*, 2001, **11**, 1501.
- 18 M. E. Noelken, P. J. Chang and J. R. Kimmel, *Biochemistry*, 1980, **19**, 1883.
- 19 D. Glover, D. J. Barlow, J. E. Pitts, I. J. Tickle, T. L. Blundell, K. Tatamoto, J. R. Kimmel, A. Wollmer, W. Strassburger and Y.-S. Zhang, *Eur. J. Biochem.*, 1985, **142**, 379.
- 20 C. Tanford, *Adv. Protein Chem.*, 1968, **23**, 544.
- 21 C. N. Pace, *Methods Enzymol.*, 1986, **131**, 266.
- 22 J. Clarke and A. R. Fersht, *Biochemistry*, 1993, **32**, 4322.